ACS APPLIED MATERIALS & INTERFACES

Research Article

www.acsami.org

Biomimetic Water-Collecting Fabric with Light-Induced Superhydrophilic Bumps

Yuanfeng Wang, Xiaowen Wang, Chuilin Lai, Huawen Hu, Yeeyee Kong, Bin Fei, and John H. Xin*

Nanotechnology Centre, Institute of Textiles and Clothing, The Hong Kong Polytechnic University, Hong Kong SAR 999077, China

Supporting Information

ABSTRACT: To develop an efficient water-collecting surface that integrates both fast water-capturing and easy drainage properties is of high current interest for addressing global water issues. In this work, a superhydrophobic surface was fabricated on cotton fabric via manipulation of both the surface roughness and surface energy. This was followed by a subsequent spray coating of TiO_2 nanosol that created light-induced superhydrophilic bumps with a unique raised structure as a result of the interfacial tension of the TiO_2 nanosol sprayed on the superhydrophobic fiber surface. These raised TiO_2 bumps induce both a wettability gradient and a shape gradient, synergistically accelerating water coalescence and water collection. The in-depth study revealed that the quantity and the distribution of the TiO_2 had a significant impact on the final water collection efficiency. This inexpensive and facilely fabricated fabric biomimicks the desert beetle's back and spider silk, which are capable of fog harvesting without additional energy consumption.

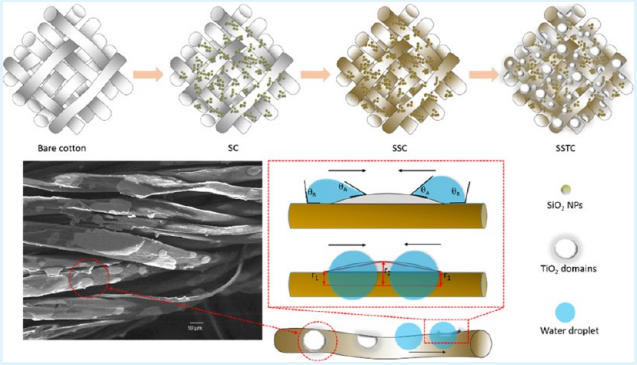

KEYWORDS: *biomimetic water collection, light-induced superhydrophilic, wettability gradient, Laplace pressure gradient, raised structure*

INTRODUCTION

Increasing attention has been paid to water-capturing technology since the 20th century because of more serious water shortage problems throughout the world, especially in those inhabited deserts and arid regions. The rainfalls in such areas are scarce, and some animals and plants rely on fog and humid air as their major sources of water. The *Stenocara* beetle from the Namib Desert can harvest water from the mist and direct the drops into its mouth because its carapace has a hydrophobic surface with a random array of hydrophilic bumps.[1−3] Cribellate spiders rely on their silks, on which alternated spindle knots and joints lead to both wettability[4,5] and curvature gradients[6,7] to collect water from humid air.[8] Additionally, some plants have also been found with water-collecting properties. For instance, *Cotula fallax*, a plant in South Africa, can collect water from fog and channel the drops to its stems by means of the hydrophobic surface and three-dimensional hierarchical structure of its leaves.[9] In some extremely droughty areas, Cactaceae species can efficiently capture fog, benefiting from the well-distributed spines and trichomes on their stems.[10] A unique water-capturing and direction behavior was also found in green bristlegrass, arising from the barb-groove structure of its bristles.[11]

Inspired by creatures in nature, some materials have been designed to realize the function of water collection from humid air.[12−15] Based on fiber materials, one-dimensional (1D) water-collecting materials imitating spider silks have been developed,[16−18] on which condensed small water drops are transported from joints to spindle knots and coalesce to form larger drops. However, these coalesced water drops collected by intricate silks or fibers can be expediently utilized by spiders rather than by human beings because they are separately distributed and difficult to collect directly and in bulk. With this consideration, the aligned barb-groove structure of some plants[10,11] or the vertically raised carapace of desert beetles,[1] which have a uniform direction, can be imitated to transport collected water into a designated device. Despite the fact that, motivated by cactus, some attempts have been made to develop spinelike water-collecting materials,[13−15] some of their synthetic procedures are too complicated to be expanded, and these approaches did not include any effective drainage system. Fortunately, the desert beetle's hydrophobic carapace with hydrophilic domains offers an idea for draining the collected water. By mimicking the desert beetle's back, a variety of strategies have been explored to fabricate 2D surfaces consisting of both hydrophobic and hydrophilic ingredients.[19−22] However, some of the approaches are still difficult to generalize because of the laborious and tedious synthetic procedures. Wang et al.[23] reported a simple route to make fabric with a superhydrophobic−superhydrophilic hybrid sur-

Received: September 21, 2015
Accepted: December 13, 2015
Published: December 13, 2015

Downloaded by INDIAN INST OF TECH ROORKEE at 01:06:45:337 on June 24, 2019
from https://pubs.acs.org/doi/10.1021/acsami.5b08941.

© 2015 American Chemical Society

DOI: 10.1021/acsami.5b08941
ACS Appl. Mater. Interfaces 2016, 8, 2950−2960

face based on the selective reactivity of thiols with Fe and Co nanoparticles. Bai et al.[24] prepared a superhydrophobic surface with star-shaped superhydrophilic patterns to create a combination of a wettability gradient and a shape gradient to improve the water collection efficiency. According to these previous reports, a water-harvesting surface should include both hydrophilic sites, where water can easily condense, and a slippery surface for water to roll off with gravity as the driving force. In the present work, inspired by both 1D spider silk and 2D beetle back, we created a superhydrophobic fabric surface with light-induced superhydrophilic bumps via a simple and efficient process that includes initial hydrophobization by SiO_2 nanoparticles (NPs) and an alkylsilane and subsequent spray coating with TiO_2 nanosol. It is worth pointing out that the deposited TiO_2 can form a raised shape because of the difficulty for sol drops to spread on the superhydrophobic cotton fibers before water evaporation. The hydrophilic spots with convex structure generate both a surface energy gradient and Laplace pressure gradient, which can accelerate the coalescence of water droplets on them. Meanwhile, by consisting of interlaced fibers, a fabric-based material provides not only channels for water drops to coalesce but also a surface from which coalesced water drops can roll off. Also, the light weight, flexibility, and low cost of the fabric make it a promising material for massive transportation and bulk production. In this work, we eliminated the inherent water-absorbing property of cotton fabric by making it superhydrophobic through both increasing the surface roughness and decreasing the surface energy.[25] To be specific, silica NPs were applied onto the cotton fabrics first to form a hierarchical structure including both microscale and nanoscale roughness. Then octadecyltriethoxysilane was applied to lower the surface energy, resulting in the superhydrophobic cotton fabric. Similar procedures to create superhydrophobic surfaces integrating NPs and hydrophobic agents have been reported previously.[26,27] The prepared superhydrophobic fabric efficiently blocks water absorption, thus improving the water drainage. Finally, TiO_2 NPs were introduced onto the pretreated fabric as hydrophilic sites via a simple spray-coating method. As demonstrated in previous reports, TiO_2 exhibits superhydrophilicity after light irradiation, which has been widely explored in changing surface wettability.[28−30] This light-induced superhydrophilicity can be utilized conveniently under the adequate sunlight of nature. In this article, the coating amount of TiO_2 was controlled by the spraying distance and the spraying time. Moreover, the effect of the size and density of hydrophilic spots distributed on the fabric on the final water collection efficiency was analyzed.

EXPERIMENTAL SECTION

Materials. Cotton fabric (twill, 202 g/m^2, provided by China Dye Ltd., Hong Kong), water glass (UNI-CHEM, 12% Na_2O and 30% SiO_2), hydrochloric acid (HCl) (Aldrich, 37%), *n*-octadecyltriethoxysilane (OTES) (Accuchem, 95%), titanium tetraisopropoxide (TTIP) (Aldrich, 97%), and acetic acid (HAc) (Aldrich, 99%) were used as received.

Synthesis of SiO_2 and TiO_2 Nanosols. The SiO_2 nanosol was prepared by the following procedures: first, water glass (10 g) was added to 100 mL of distilled water under magnetic stirring at room temperature for 10 min, and 2 M HCl solution was added dropwise to the water glass solution under magnetic stirring until the pH of the mixture reached 8−9.

The TiO_2 nanosol was prepared by hydrolysis of a TTIP hydrosol. First, TTIP (40 g) was added dropwise into 100 mL of distilled water solution containing HAc (0.5 wt %) and HCl (1 wt %) under vigorous mechanical stirring. The prepared TTIP hydrosol was then dropped slowly with simultaneous addition of of water at 83−90 °C for 4 h to produce a milklike sol. Subsequently, the sol was cooled to 60 °C and stirred violently for 15 h until a transparent bluish sol was obtained. Finally, the mixture was cooled in air to room temperature and aged for 2 weeks, resulting in the final TiO_2 nanosol, which had a TiO_2 solid content of 10 wt %. The above TiO_2 sol was diluted 10-fold before use.

Fabrication of Superhydrophobic Fabric with Light-Induced Superhydrophilic Domains. The cotton fabrics were immersed into the prepared SiO_2 sol for 1 min and then padded with an automatic padder at a pressure of 2 kg/cm^2 to ensure a uniform coating of SiO_2 NPs. After they were dried at 80 °C for 3 min, the fabrics were dipped in an OTES/ethanol solution with an OTES concentration of 5 wt % for 30 min. Then the fabrics were washed using ethanol and dried at 80 °C for 3 min, followed by curing at 160 °C for another 3 min.

Spraying equipment (HD-130, RUIYI, Taiwan) was applied to spray the TiO_2 nanosol onto the as-prepared superhydrophobic cotton fabrics. The spray-coating time was controlled at 5 s for all of the samples, and the distance was varied at 3, 5, 7, 9, 11, 13, and 15 cm to make different samples. A simultaneous heat treatment using a hot plate was conducted during the spraying process to facilitate the evaporation of water. After the spray coating, the cotton fabrics were dried at 80 °C for 3 min.

For comparison, a piece of pristine cotton fabric was also treated directly by spray coating with the TiO_2 sol according to the above procedures (with a spraying distance of 11 cm).

Characterization. Scanning electron microscopy (SEM) on a Jeol 6490 microscope was used to observe the bare cotton fabric (bare-C) and cotton fabrics treated with SiO_2 NPs, SiO_2 NPs/OTES, SiO_2 NPs/OTES/TiO_2, and only TiO_2 (defined as SC, SSC, SSTC, and TC, respectively). Before they were applied on fabrics, SiO_2 NPs and TiO_2 NPs were observed by transmission electron microscopy (TEM) on a Jeol JEM-2011 microscope. To make SiO_2 and TiO_2 NPs, 10 μL of SiO_2 or TiO_2 sol with a concentration of 0.1 wt % was dripped onto the copper mesh and dried. X-ray diffraction (XRD) using a Rigaku SmartLab diffractometer was performed to study the crystallinity of TiO_2. The morphology of bare-C and SC were recorded by atomic force microscopy (AFM) on a Veeco NanoScope V microscope in tapping mode. X-ray photoelectron spectroscopy (XPS) using a Sengyang SKL-12 spectrometer was performed to distinguish the surface chemical compositions of SC, SSC, and SSTC. The elementary composition and distribution were further studied using an energy-dispersive X-ray spectroscopy (EDX) detector attached to the scanning electron microscope. Water contact angles (WCAs) for all of the samples were measured on an OCA20 instrument (Data Physics). The thermal weight losses of SSTC samples with different spraying distances were investigated by thermogravimetric analysis (TGA) using a PerkinElmer Diamond thermogravimetric analyzer.

Water Collection Measurement. An artificial fog flow (200 mL/h) horizontally generated by an ultrasonic humidifier (Midea, S20U-A) was used to simulate natural fog. All of the prepared samples (bare-C, TC, SSC, and SSTC with various spraying distances) having a uniform size of 3 cm × 3 cm were first exposed to UV irradiation (by four UV lamps with irradiation wavelength of 365 nm and UV intensity of 0.46 mW/cm^2 for each lamp) for 30 min (the same results could be obtained by 1 h of sunlight irradiation with a UV intensity of ∼1 mW/cm^2) and subsequently fixed vertically with respect to the direction of fog flow at room temperature (23 °C). A beaker was placed under the sample to receive the collected water. The time was recorded when the first water drop dripped off each fabric sample. Also, the weight of the first water drop was measured. Finally, the water-collecting capacity of each sample was evaluated after 30 and 60 min. Moreover, in order to observe the water condensation and coalescence process, a fog flow was directed vertically over the horizontally placed fabrics. A digital camera was used to capture pictures.

Stability and Durability Study. The durability of the superhydrophobic coating and TiO_2 bumps was studied by repeated water collection and abrasion tests. One cycle of water collection included a prior UV irradiation for 30 min, 1 h of water-collecting process using the method previously described, and drying in air. The WCA and

DOI: 10.1021/acsami.5b08941
ACS Appl. Mater. Interfaces 2016, 8, 2950−2960

Scheme 1. Illustration of the Fabrication Process for SC, SSC, and SSTC Fabrics

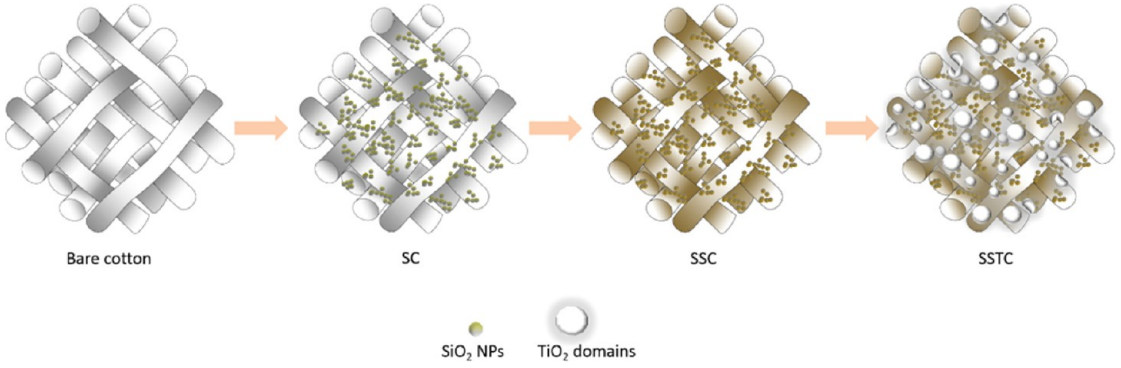

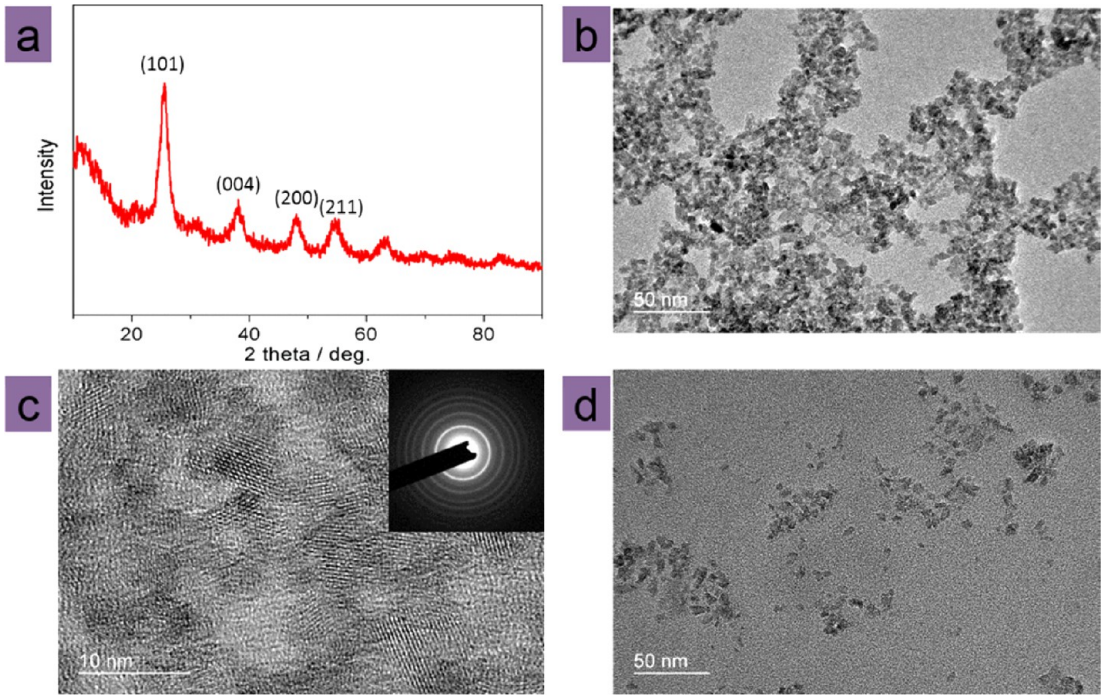

Figure 1. (a–c) Characterization of TiO_2 NPs by (a) XRD, (b) low-resolution TEM, and (c) high-resolution TEM. (d) TEM observation of SiO_2 NPs. The inset in (c) is the SAED pattern for the observed TiO_2 NPs.

water collection performance of SSTC-11 fabric were recorded after 5, 10, and 15 cycles. SEM and EDX mapping were used to observe the surface morphology and element distribution, respectively, after 15 cycles of water collection. The abrasion test was conducted using a Martindale abrasion tester based on the ASTM D4966-12 standard. After 100 and 500 cycles of friction, the WCA (after UV irradiation), water collection performance, SEM image, and EDX mapping were recorded. Two types of acidic fog flow were made from water solutions with pH values of 3 and 5 containing H_2SO_4 and HNO_3 (1.9:1 w/w) to simulate acid rain.[31] The water collection stability and morphology of SSTC-11 fabric was studied under an acidic fog flow for 15 cycles. The water collection performance of the prepared SSTC-11 fabric was also investigated at different temperatures (20, 25, and 40 °C) by conducting the experiments in a constant-temperature laboratory, a common laboratory without air conditioning, and an oven, respectively.

RESULTS AND DISCUSSION

The fabrication procedure from bare-C to SSTC is demonstrated in Scheme 1. SiO_2 NPs were first synthesized beforehand by a sol–gel process with water glass as the precursor and then applied onto the fabric via a simple dip–pad–dry method. Then the SC was treated with OTES to form a superhydrophobic SSC fabric. Finally, the TiO_2 sol was sprayed onto the surface of the SSC fabric to create raised hydrophilic domains after drying at 80 °C.

In order to investigate the crystallinity of titania particles by XRD, the titania solid powders were extracted from the TiO_2 sol. As shown in Figure 1a, the characteristic peaks of TiO_2 in the anatase phase (25.4°, 37.8°, and 48.1°) were detected in the XRD pattern. Anatase TiO_2 has been reported to have strong photocatalytic properties and light-induced superhydrophilicity.[28] The light-responsive wettability change of TiO_2-treated cotton fabric (TC) was studied. As shown in Figure S1, the introduction of TiO_2 lengthened the time to wick the water droplet, indicating a decrease in the hydrophilicity of the cotton fabric. However, after UV irradiation for 30 min (or sunlight irradiation for 1 h), a much shorter time was needed for the WCA to become 0° than before UV irradiation, indicating a wettability transformation of TiO_2 to superhydrophilicity. It should be noted that this superhydrophilic status can be maintained for at least 12 h in the absence of light (top row in Figure S2), which can ensure good fog capture the next

DOI: 10.1021/acsami.5b08941
ACS Appl. Mater. Interfaces 2016, 8, 2950–2960

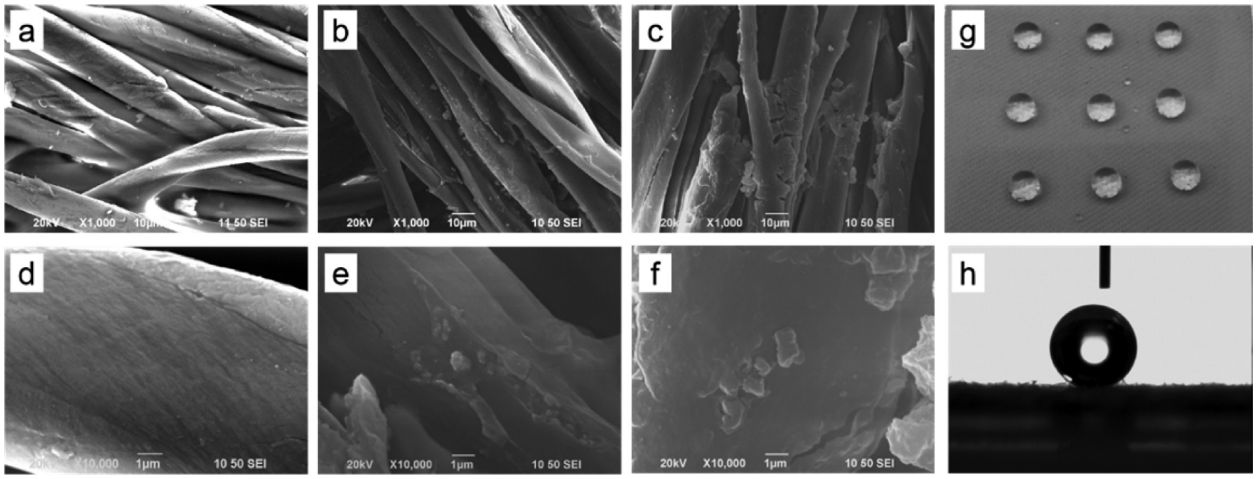

Figure 2. (a–f) SEM images of (a, d) bare-C, (b, e) SC, and (c, f) SSC fabrics at different magnifications (a–c, 1000×; d–f, 10000×). (g) Optical image of water macrodroplets on the as-prepared SSC fabric. (h) WCA of ~155.6° on the as-prepared SSC fabric.

morning even after a whole night of storage. After about 48 h of dark storage, however, TiO_2 turns hydrophobic (bottom row in Figure S2). Hence, on cloudy and rainy days, TiO_2 bumps can turn hydrophobic and have a better resistance to damage by flush rainwater. TEM was also performed to characterize the TiO_2 and SiO_2 NPs, which were deposited from TiO_2 and SiO_2 nanosols with concentrations of 0.1 wt %. From Figure 1c, a diameter of around 10 nm could be measured for each TiO_2 NP, but an aggregation phenomenon of TiO_2 NPs could also be found in the absence of water (Figure 1b). The aggregation instinct of TiO_2 NPs is conductive to the formation of scattered hydrophilic TiO_2 domains. Conversely, SiO_2 NPs had much better dispersibility after the evaporation of water (Figure 1d), which may be responsible for the homogeneous coating of SiO_2 NPs and the even roughness increase on the SC fabric.

SEM was conducted to observe the surfaces of bare-C, SC, and SSC (Figure 2a–f). In Figure 2a,d, the flat, smooth surface of bare cotton fiber can be seen. After padding with the SiO_2 sol and drying, the surface of the cotton fiber was covered with a layer of SiO_2 NPs, which introduced nanoscale roughness onto the surface (see the AFM images of bare-C and SC in Figure S3a,b, respectively). The increase in the surface roughness can maximize the surface wettability levels.[25] Therefore, after treatment with OTES, which has low surface energy, the fabric surface turned superhydrophobic (Figure 2g) with a WCA of about 155.6° (Figure 2h). This superhydrophobic fabric surface ensures efficient water drainage by accelerating the roll off of the water droplets.

After the fabrication of the superhydrophobic fabric, hydrophilic domains were introduced simply by spraying TiO_2 sol onto the as-formed superhydrophobic surface. The coating amount of TiO_2 and the domain size was generally determined by the spraying distance. Specifically, SSTC samples fabricated with different spraying distances of 3, 5, 7, 9, 11, 13, or 15 cm are denoted as SSTC-3, SSTC-5, SSTC-7, SSTC-9, SSTC-11, SSTC-13, and SSTC-15, respectively. It should be noted that the spraying time for all the SSTC samples was maintained the same (5 s). The spraying process is demonstrated in Scheme 2. A longer spraying distance can lead to smaller and more scattered TiO_2 domains and a lower TiO_2 coating percentage, which is demonstrated in detailed in the following section. The distribution of the light-induced superhydrophilic domains has a complicated influence on the water collection efficiency of SSTC fabrics, which will be discussed in the subsequent section.

Scheme 2. Illustration of Spray Coating of TiO_2 Sol onto SSC Fabrics with Variation of the Distance between the Nozzle and the Fabric

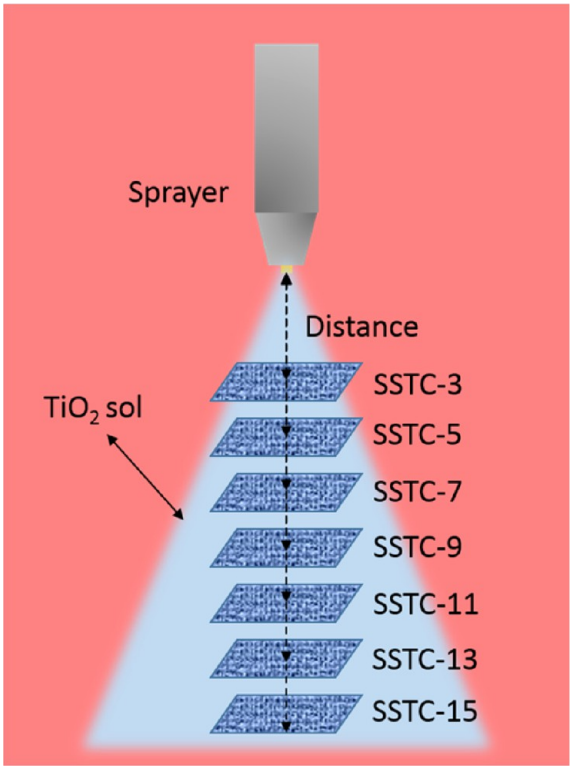

The elemental composition and distribution of the prepared samples were studied by XPS and EDX. The elementary change during the synthesis process from SC fabric to SSTC fabric was recorded by XPS curves. As shown in Figure S4a,b, the Si 2p peak was detected on the SC fabric at around 103.4 eV, indicating the successful preparation of SiO_2 and coating of SiO_2 on the cotton fabric. After treatment with OTES, the C 1s peak intensity relative to that of the O 1s peak was greatly increased because of the existence of the long aliphatic carbon chain of OTES. Upon subsequent spray coating of the TiO_2 sol

DOI: 10.1021/acsami.5b08941
ACS Appl. Mater. Interfaces 2016, 8, 2950–2960

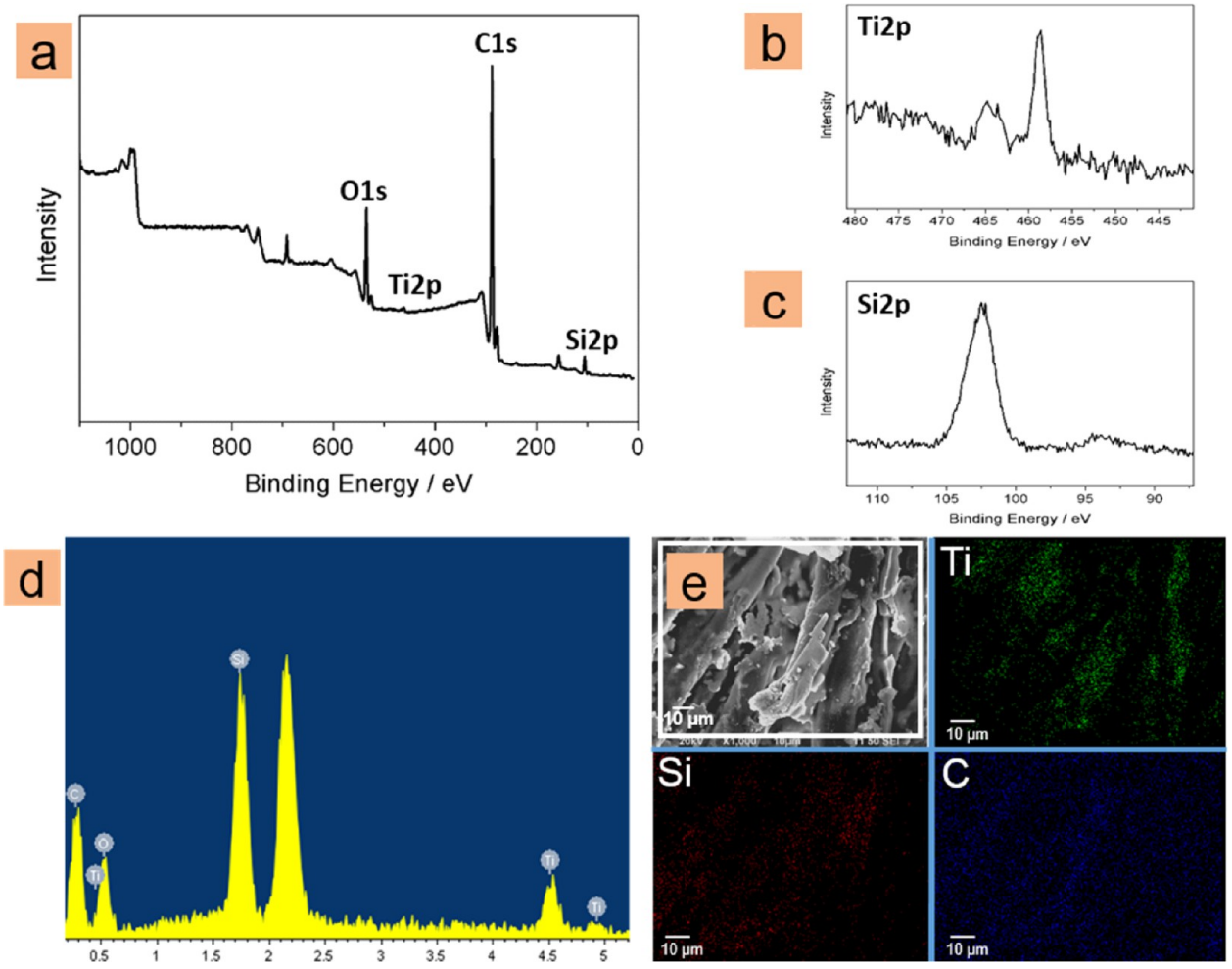

Figure 3. Elemental composition and distribution of the as-prepared SSTC fabric. (a–c) XPS survey spectrum, high-resolution Ti 2p spectrum, and high-resolution Si 2p spectrum, respectively. (d) EDX spectrum of the resultant SSTC fabric. (e) EDX maps of Ti, Si, and C on the SSTC fabric corresponding to the SEM image.

(Figure 3a–c), the Ti $2p_{3/2}$ peak (Figure 3b) started to appear at around 458.5 eV, denoting the presence of TiO_2 on the fabric. To further demonstrate the composition of the SSTC fabric (SSTC-11), the EDX spectrum and maps are given in Figure 3d,e. The results confirm the presence of C, O, Ti, and Si and display the distributions of Ti, Si, and C. It can be seen that Si and C are both uniformly distributed, as shown in the corresponding SEM image, while Ti is distributed as scattered domains with irregular shapes. The discrete distribution of TiO_2 is attributed to the superhydrophobic surface, on which the sprayed TiO_2 sol beads up; this is the key factor in fog trapping and coalescence.

To study the water collection efficiency, bare-C, TC, SSC, and SSTC were compared with respect to the weight of collected water after 30 and 60 min. The starting time for collection and the weight of the first drop off each sample were also recorded. Before water collection, all of the samples were exposed to UV light (365 nm) for 30 min, and the comparison of the water collection results is presented in Figure 4. As shown in Figure 4a,b, the SSTC samples have a generally higher water collection efficiency than bare-C, TC, and SSC. The poor water collection capacities of bare-C and TC can be explained by their inherent hydrophilic and water-absorbing properties. Condensed water on bare-C or TC can wet and saturate the fabric before dripping, so the starting times for collection of bare-C and TC are much longer than for the other samples with superhydrophobic modification. Furthermore, Figure 4c,d shows that TC took the longest time until the first drop dripped, and the weight of its first water drop was the largest. This can be attributed to the superhydrophilicity of the TiO_2-treated cotton fabric after UV irradiation, which leads to high water absorption capacity and strong water adhesion property and thus an inefficient water collection property.

On the contrary, the superhydrophilic property of TiO_2 can play a positive role in water collection when combined with superhydrophobic substrate. After the introduction of TiO_2 domains, the water collection efficiency of the superhydrophobic fabrics was generally increased, except for SSTC-15 (see Figure 4b), indicating an increase in water condensation on the surfaces with superhydrophilic domains. However, the presence of more hydrophilic domains does not mean higher water collection efficiency. The incorporation of too much hydrophilic ingredient destroys the original superhydrophobicity of the fabric, which may lead to poor water collection property, such as in the case of SSTC-3, SSTC-5, and SSTC-7 (Figure 4b). The effect of the amount of TiO_2 coating on the hydrophobicity of the fabric is indicated in Figure 5. After UV irradiation, SSTC fabrics with more TiO_2 coating had a higher degree of WCA decrease. As for SSTC-3–SSTC-7 with too much TiO_2 coverage, a hydrophilic property appeared after UV

DOI: 10.1021/acsami.5b08941
ACS Appl. Mater. Interfaces 2016, 8, 2950–2960

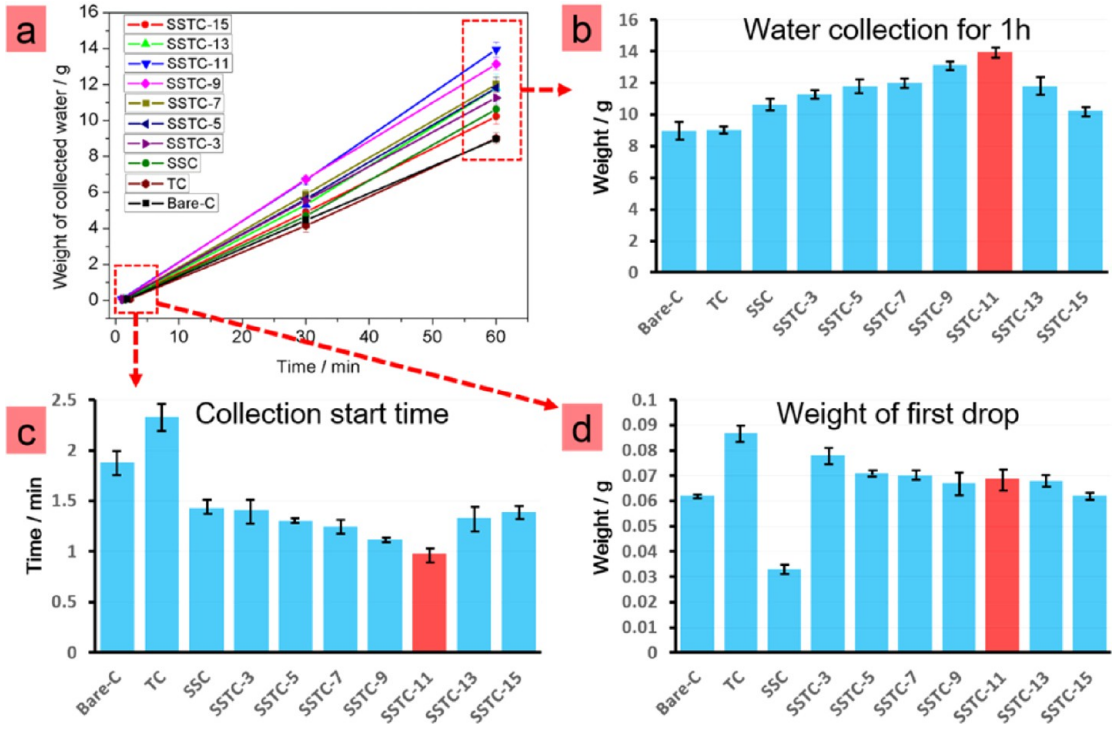

Figure 4. Water collection performance of various fabrics. (a) Water collection amount for each sample along with the collection time. (b) Total amount of collected water for each sample after 1 h. (c) Starting time for collection, i.e., the time needed for each fabric to drip the first water drop in the fog environment. (d) Weight of the first water drop at the starting time for collection.

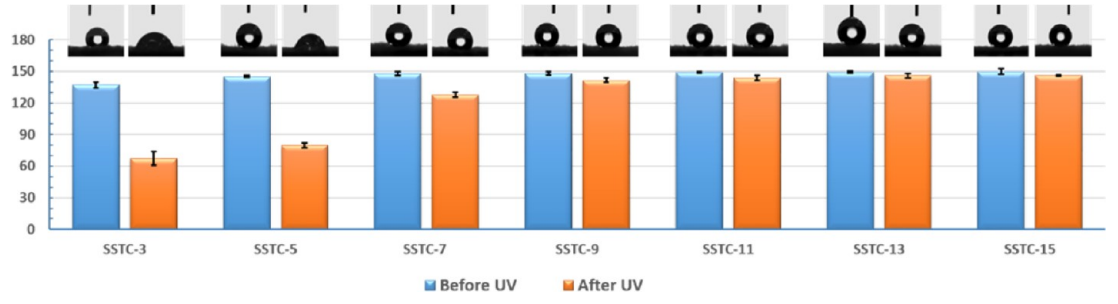

Figure 5. WCAs of SSTC fabrics with various spraying distances before and after UV irradiation. The insets above the histogram show the corresponding shapes of water drops on the fabrics.

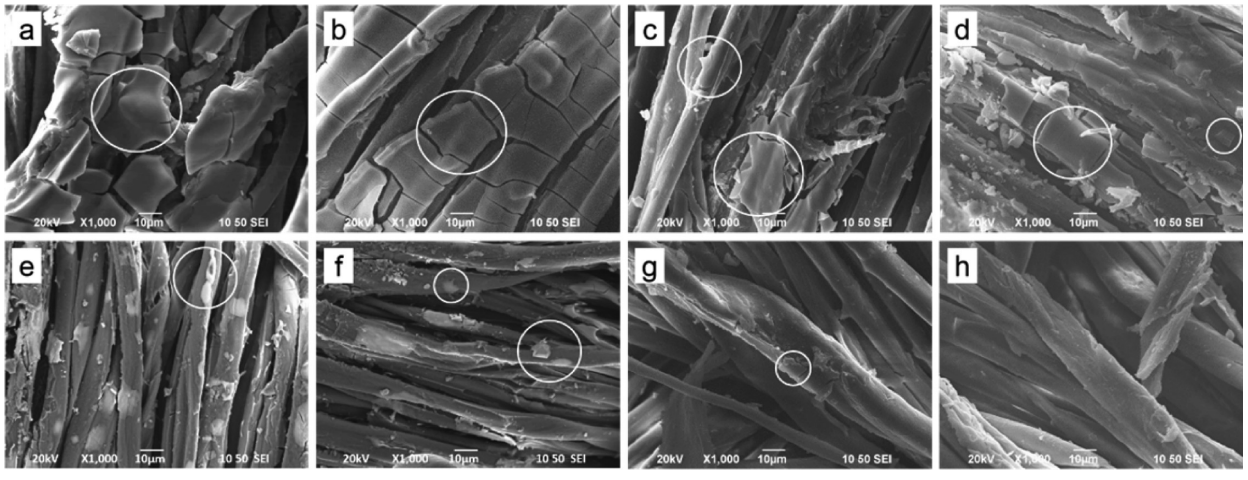

Figure 6. SEM images of (h) TC and (a–g) SSTC with various spraying distances: (a) SSTC-3; (b) SSTC-5; (c) SSTC-7; (d) SSTC-9; (e) SSTC-11; (f) SSTC-13; (g) SSTC-15. The white circles in (a–g) mark the TiO_2 domains. No obvious TiO_2 domains can be seen in the TC sample (h).

DOI: 10.1021/acsami.5b08941
ACS Appl. Mater. Interfaces 2016, 8, 2950–2960

exposure. However, when the spraying distance was more than 9 cm, the decline in superhydrophobicity seemed less obvious. It should be noted that the SSTC-11 fabric, which had the best water collection efficiency among all the samples (see Figure 4b), exhibited a WCA close to 150° (Figure 5), indicating good maintenance of the superhydrophobic property. The gradual decrease in the WCA with increasing UV irradiation time was also recorded on the SSTC-11 fabric (see Figure S5a). The corresponding ascent in the amount of water collected (Figure S5b) indicates the important role that the superhydrophilic TiO_2 bumps play in water pinning. In summary, the water collection efficiency is mainly determined by the combined effect of the hydrophobicity of the surface and the amount of hydrophilic ingredient. To be specific, an efficient water collection surface should possess not only sufficient superhydrophilic sites to adhere and fix fog droplets but also an integral superhydrophobic property to accelerate the rolling of water drops.

SEM images of SSTC fabrics with various spraying distances are displayed in Figure 6a–g. The top surfaces of SSTC-3 and SSTC-5 are almost fully covered by contiguous titania bumps, each of which extends across the width of one or two fibers (Figure 6a,b). With increasing spraying distance, the TiO_2 bumps seem less dense on surfaces of SSTC-7 and SSTC-9 but still have large sizes with a width equal to that of the fiber (Figure 6c,d). When the spraying distance reaches 11 and 13 cm, smaller and scattered titania domains appear with diameters ranging from one to a few tens of micrometers (Figure 6e,f). Finally, on the surface of the SSTC-15 fabric, very scarce titania domains could be seen (Figure 6g), which may be responsible for its poor water collection performance because of the insufficient number of hydrophilic sites on which fog can condense. Additionally, an SEM image of the TC fabric is shown in Figure 6h for a better comparison with the SSTC fabrics. No raised TiO_2 domains could be found on the surface of the TC fabric because the sprayed sol can spread evenly on the pristine cotton fabric.

In order to further study the relationship between the spraying distance and the coating amount of TiO_2, TGA was performed to study the weight percentage of TiO_2 in the SSTC fabrics with a series of spraying distances (Figure 7). Bare-C and SSC samples were chosen as references. Pyrolysis of the samples started at about 350 °C, corresponding to the decomposition of cellulose fibers.[32,33] Finally, the weight gain percentage of TiO_2 on each SSTC fabric was calculated from the difference between the residue percentages of the SSC and SSTC fabrics. As can be seen from Figure 7, a shorter spraying distance indicates a higher percentage of TiO_2 coating. This result was also supported by EDX detection of the Ti content on the fabric surface, as shown in Figure S6. Specifically, with the TiO_2 gain percentage of ~0.92% (by TGA), the SSTC-11 sample achieved the best water collection performance in our study as a result of its sufficient number of hydrophilic sites with no obvious damage effect on the integral superhydrophobicity.

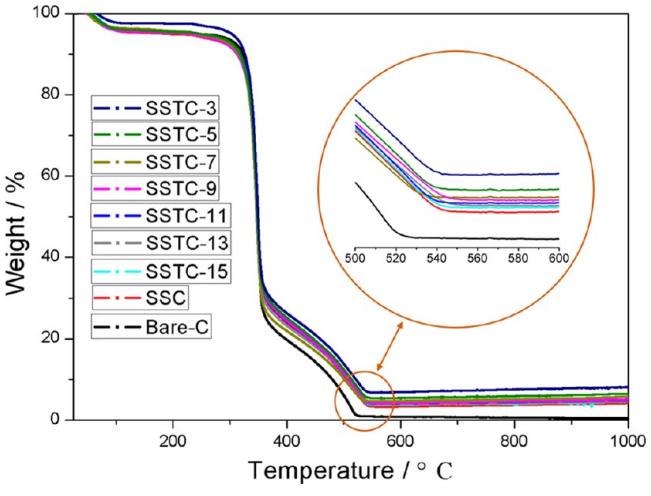

Figure 7. TGA spectra of SSTC fabrics with various spraying distances, with the bare-C and SSC fabrics as references.

To investigate how the superhydrophilic TiO_2 domains influence the water-condensing velocity on a superhydrophobic fabric surface, the water condensation and coalescence process of SSTC-11 was recorded using a digital camera discretely from 30 s to 4 min with the SSC and TC fabrics as references. A prior UV light exposure was conducted for 30 min to switch the TiO_2 coating to be superhydrophilic. A fog flow (200 mL/h) was then directed vertically onto the horizontally placed fabrics. As shown in Figure 8a, during the fog condensation process, no spherical water droplets can be formed on the TC fabric because water easily spreads on its superhydrophilic surface with strong water absorption. In contrast, coalesced water forms visible spherical droplets on the integral superhydrophobic surfaces of the SSC and SSTC-11 fabrics, as shown in Figure 8b,c, respectively. However, in the presence of superhydrophilic spots, SSTC-11 fabric harvested more and larger water droplets than SSC fabric with the same harvesting time. This fog-pinning and overall superhydrophobic property of the SSTC-11 fabric can well explain the results shown in Figure 4c,d, namely, that it had the earliest starting time for water collection and a large weight of the first drop collected.

The mechanism of how the sprayed TiO_2 bumps accelerate water condensation and coalescence on the SSTC fabrics was analyzed in detail (see Figure 9). After light irradiation, the sprayed TiO_2 bump becomes superhydrophilic, which means that it has a much higher apparent surface energy and smaller WCA than the surrounding superhydrophobic fiber. The driving force generated by the surface energy gradient can be calculated as[4,5]

$$F = \int_{L_f}^{L_t} \gamma(\cos\theta_A - \cos\theta_R)\, dl \quad (1)$$

where γ is the surface tension of water, θ_A and θ_R represent the advancing and receding contact angles, respectively, during the movement of the water drop at the boundary between the TiO_2 bump and the fiber surface ($\theta_A < \theta_R$; Figure 9b), and l is the integration variable along the length from the fiber surface (L_f) to the TiO_2 bump (L_t). As predicted by eq 1, the water droplets will move from the superhydrophobic fiber surface to the superhydrophilic TiO_2 bump, driven by the surface gradient. Moreover, there is another possible driving force generated by the Laplace pressure gradient. In Figures 6 and 9a, raised TiO_2 domains can be seen because of the difficulty of spreading of the TiO_2 sol droplets on the superhydrophobic fabric. The raised TiO_2 spots lead to a local increase in the fiber radius (from r_1 to r_2 in Figure 9c) and can be viewed as two partial conical shapes. The Laplace pressure gradient (ΔP), which arises from the curvature gradient, can be approximately calculated as[6,8]

DOI: 10.1021/acsami.5b08941
ACS Appl. Mater. Interfaces 2016, 8, 2950–2960

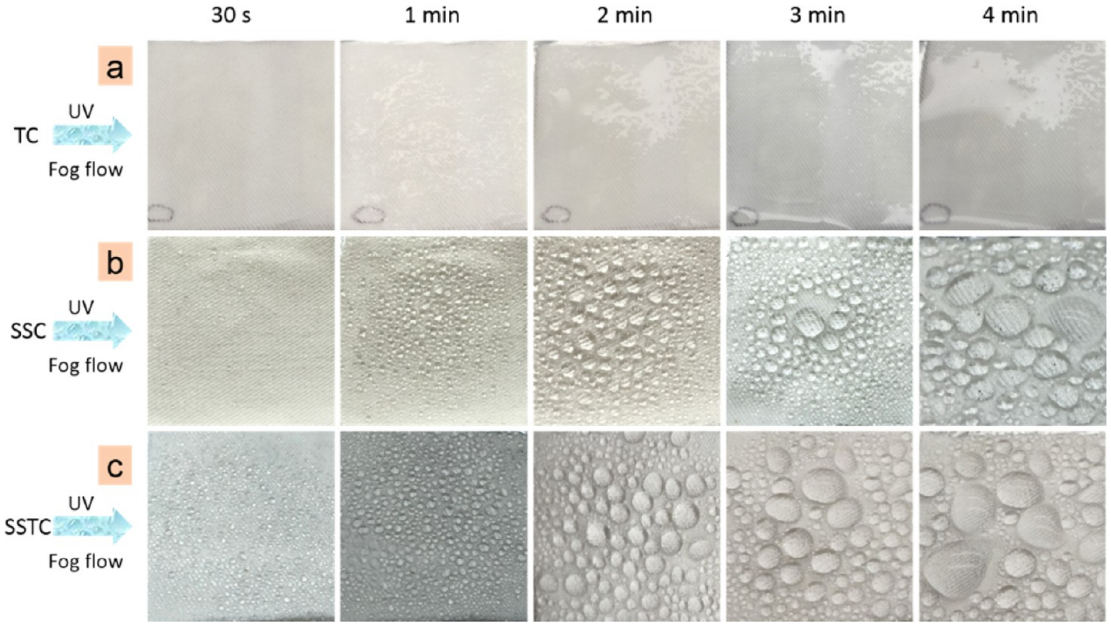

Figure 8. Water condensation and coalescence process as a function of time on the (a) TC, (b) SSC, and (c) SSTC-11 fabrics (the UV treatment was conducted before atomization of the fog).

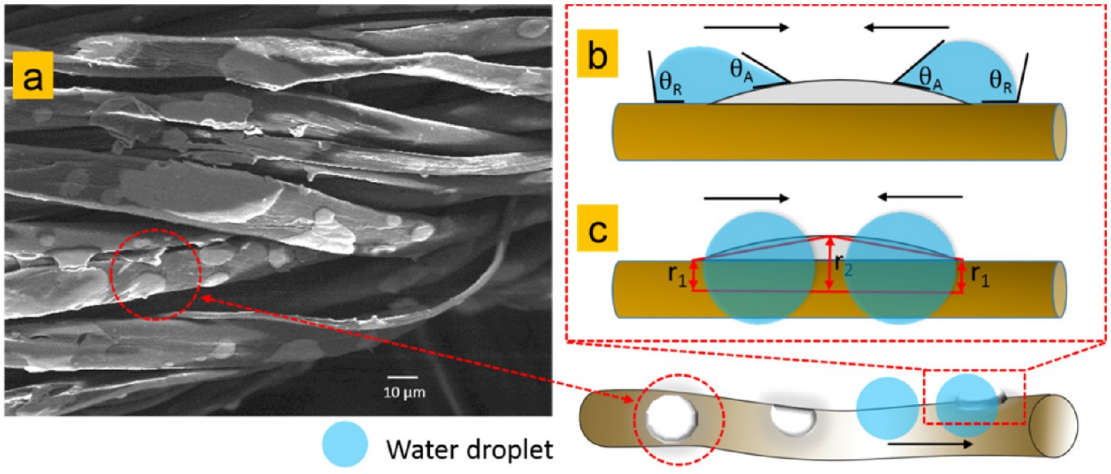

Figure 9. Structure and distribution of raised TiO_2 domains on SSTC-11 fabric and the mechanism of directional water coalescence. (a) SEM image showing the shape and distribution of raised TiO_2 domains on SSTC-11 fabric. (b) Illustration of the driving force caused by the surface energy difference between a superhydrophilic TiO_2 domain and the superhydrophobic fiber. (c) Illustration of the Laplace pressure gradient between the fiber and the thickened TiO_2 area.

$$\Delta P = -\int_{r_1}^{r_2} \frac{2\sigma\gamma}{(r + R_0)^2} \sin\beta \, dz \qquad (2)$$

where r denotes the local mean radius of the fiber, β denotes half of the apex angle of the conical shape, z is the integration variable along the diameter of the fiber, and σ is the proportion of the TiO_2 domain relative to the whole cone (because the TiO_2 domain partially encircles the local fiber surface, the formed cone is not integrated, i.e., $\sigma < 1$). Overall, as a result of these two cooperative driving forces, the surface energy gradient and the Laplace pressure gradient, water droplets are more prone to coalesce from the superhydrophobic fiber to the superhydrophilic TiO_2 domains.

Besides the significance of the water capture (condensation and coalescence) process, drainage of the captured water is also important. An effective water drainage system means larger water release in a shorter time. To simulate the growth and release of water drops during the water collection process, we added a water drop on each horizontal UV-irradiated fabric (the bottom side of the fabric was adhered to a glass slide using double-sided adhesion tape) and then rotated the fabric to upright. The growth of the water drop was conducted by using a microsyringe to add water to the initial drop. The growth process was recorded using a digital camera discretely until the drop started to roll off. Figure 10a–c shows the different mechanisms of water drainage for the TC, SSC, and SSTC fabrics, while Figure 10d–f depicts their corresponding simulations displayed by photographs. Figure 10a,d displays the poor water drainage on the superhydrophilic TC fabric. Water undergoes a thorough spread and is absorbed by the fabric before it can drip down from the bottom end (Figure 10d-4). Also, the strong adhesion force between water drops and the superhydrophilic surface makes it difficult for water to drip down. Therefore, the drainage time is long because the

DOI: 10.1021/acsami.5b08941
ACS Appl. Mater. Interfaces 2016, 8, 2950–2960

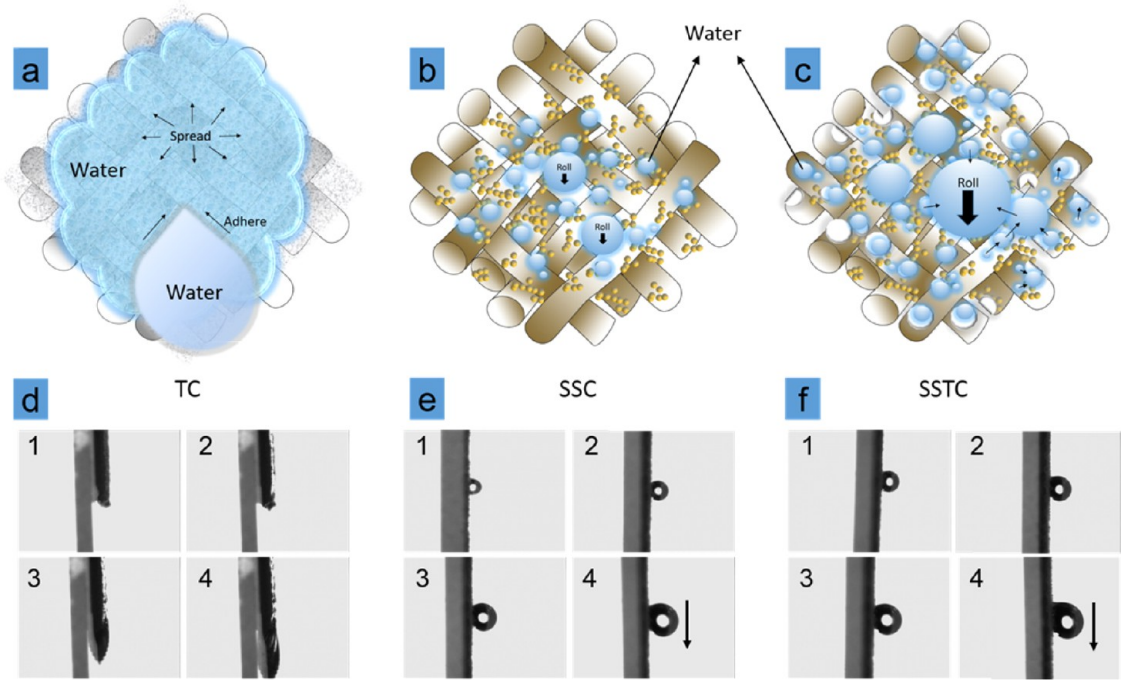

Figure 10. (a–c) Graphic illustrations of the different water drainage mechanisms on the (a) TC, (b) SSC, and (c) SSTC fabrics. (d–f) Photographs of simulations of water growth and rolling processes corresponding to the different drainage mechanisms on the (a) TC, (b) SSC, and (c) SSTC fabrics.

captured water needs to spread thoroughly and coalesce to be large enough to overcome the strong adhesion force, which can also explain the results for TC shown in Figure 4c,d. In contrast, water drainage from the SSC and SSTC fabrics is favored because of their overall superhydrophobic property. Water drops form almost perfect spheres with a tiny contact area with the fabric surface and a low adhesion force, which may lead to rapid water release (Figure 4c,d). It should be noted that the SSTC fabric (Figure 10f) had a little higher critical roll-off volume than the SSC fabric (Figure 10e), which can be attributed to the slight reduction in hydrophobicity caused by incorporation of TiO_2. However, it does not lower the overall water collection efficiency (Figure 4b) because the TiO_2 bumps accelerate the pinning and growing of water drops on the fabric surface, as discussed above. Overall, the as-prepared SSTC fabric exhibits an effective water collection function due not only to the enhanced water capture and growth but also to efficient drainage.

Finally, the stability and durability of the SSTC-11 fabric was studied by repeated water collection and abrasion tests. As shown in Figure S7a,b, there was no obvious impairment in the WCA or water collection performance even after 15 cycles of water collection repetition. This is attributed to the good conservation of the silica/silane superhydrophobic coating and the raised TiO_2 bumps, which can be observed in the SEM image and EDX maps shown in Figure S7c–e. Even in an acidic fog flow, stable water collection performance and good retention of the functional coating (after 15 cycles) were observed (Figure S8). Abrasion tests were also conducted to evaluate the adhesion strength of the functional coating against friction during transportation. It can be seen from Figure S9 that 100 cycles of friction generated scarcely any damage to the surface coating and the WCA (after UV irradiation). Although 500 cycles of friction caused a slight decrease in the density of TiO_2 bumps, it is hardly likely that products will undergo such high-strength friction in practical transport. Hence, the adhesion between the cotton fabric and the surface finishing can withstand repetitive water (including acidic water) flush and friction, which ensures stable water collection performance. In addition, the impact of temperature on the water collection performance was also investigated. As shown in Figure S10, with increasing temperature a decrease in the water collection occurs, which might be attributed to the easier condensation of fog at lower temperature and the faster evaporation of water (including fog and the collected water) at higher temperature. Therefore, in areas at high latitudes where the morning temperature is very low, better water collection performance of the as-prepared SSTC fabric can be expected.

CONCLUSION

An efficient water-collecting fabric with a superhydrophobic surface integrated with light-induced superhydrophilic bumps has been successfully fabricated by a simple method. As a result of the bead-forming feature of a TiO_2 sol on a superhydrophobic surface, raised TiO_2 bumps are obtained, which may provide a surface energy gradient and Laplace pressure gradient that cooperatively accelerate the directed coalescence of water droplets. The spraying distance of the TiO_2 sol (at fixed spraying time) had significant effect on the water collection efficiency through control of the coating amount and distribution of TiO_2. In order to attain efficient water collection, a sufficient number of scattered TiO_2 bumps should be formed on the base with overall superhydrophobicity. The as-prepared SSTC fabric can thereby be regarded as an inspiration of both 1D spider silk and 2D beetle back with water-collecting function. Simply triggered by sunlight, a sustainable energy source, the superhydrophilicity of TiO_2 can be achieved without additional effort, which may provide ideas leading to the development of smart water collection devices. Furthermore, the self-cleaning or antibacterial property

DOI: 10.1021/acsami.5b08941
ACS Appl. Mater. Interfaces 2016, 8, 2950–2960

of TiO_2 makes it a more competitive material for application in water harvesting and recycling.

■ ASSOCIATED CONTENT

Supporting Information

The Supporting Information is available free of charge on the ACS Publications website at DOI: 10.1021/acsami.5b08941.

Illustration of the light-induced superhydrophilicity of TiO_2; illustration of the wettability change of TiO_2 after storage in the dark for various times; AFM images of the bare-C and SC fabrics; XPS spectrum of the prepared SC and SSC fabrics; SEM, EDX, WCA, and water collection performance of SSTC-11 fabric after 15 cycles of water collection repetition (under neutral and acidic fog flow) and abrasion tests for 100 and 500 cycles; and water collection performances at different ambient temperatures (PDF)

■ AUTHOR INFORMATION

Corresponding Author

*Fax: +86-852-2766-6474. E-mail: tcxinjh@polyu.edu.hk.

Author Contributions

The manuscript was written through contributions of all authors. All authors have given approval to the final version of the manuscript.

Notes

The authors declare no competing financial interest.

■ ACKNOWLEDGMENTS

The authors gratefully acknowledge the financial support from The Hong Kong Polytechnic University Internal Fund (project code PolyU G-YK50). We acknowledge Mr. Ben Wang for assistance with AFM analysis and Ms. Zhaoyu Zhang for the drawing of the fibrous textile matrix.

■ REFERENCES

(1) Parker, A. R.; Lawrence, C. R. Water capture by a desert beetle. *Nature* **2001**, *414*, 33−34.

(2) Seely, M. K.; Hamilton, W. J. Fog Catchment Sand Trenches Constructed by Tenebrionid Beetles, Lepidochora, from Namib Desert. *Science* **1976**, *193*, 484−486.

(3) Seely, M. K. Irregular Fog as a Water Source for Desert Dune Beetles. *Oecologia* **1979**, *42*, 213−227.

(4) Chaudhury, M. K.; Whitesides, G. M. How to Make Water Run Uphill. *Science* **1992**, *256*, 1539−1541.

(5) Daniel, S.; Chaudhury, M. K.; Chen, J. C. Fast drop movements resulting from the phase change on a gradient surface. *Science* **2001**, *291*, 633−636.

(6) Lorenceau, E.; Quere, D. Drops on a conical wire. *J. Fluid Mech.* **1999**, *510*, 29−45.

(7) Bai, H.; Tian, X. L.; Zheng, Y. M.; Ju, J.; Zhao, Y.; Jiang, L. Direction Controlled Driving of Tiny Water Drops on Bioinspired Artificial Spider Silks. *Adv. Mater.* **2010**, *22*, 5521−5525.

(8) Zheng, Y. M.; Bai, H.; Huang, Z. B.; Tian, X. L.; Nie, F. Q.; Zhao, Y.; Zhai, J.; Jiang, L. Directional water collection on wetted spider silk. *Nature* **2010**, *463*, 640−643.

(9) Andrews, H. G.; Eccles, E. A.; Schofield, W. C. E.; Badyal, J. P. S. Three-Dimensional Hierarchical Structures for Fog Harvesting. *Langmuir* **2011**, *27*, 3798−3802.

(10) Ju, J.; Bai, H.; Zheng, Y. M.; Zhao, T. Y.; Fang, R. C.; Jiang, L. A multi-structural and multi-functional integrated fog collection system in cactus. *Nat. Commun.* **2012**, *3*, 1247.

(11) Xue, Y.; Wang, T.; Shi, W. W.; Sun, L. L.; Zheng, Y. M. Water collection abilities of green bristlegrass bristle. *RSC Adv.* **2014**, *4*, 40837−40840.

(12) Chen, Y.; Zheng, Y. M. Bioinspired micro-/nanostructure fibers with a water collecting property. *Nanoscale* **2014**, *6*, 7703−7714.

(13) Heng, X.; Xiang, M. M.; Lu, Z. H.; Luo, C. Branched ZnO Wire Structures for Water Collection Inspired by Cacti. *ACS Appl. Mater. Interfaces* **2014**, *6*, 8032−8041.

(14) Ju, J.; Xiao, K.; Yao, X.; Bai, H.; Jiang, L. Bioinspired Conical Copper Wire with Gradient Wettability for Continuous and Efficient Fog Collection. *Adv. Mater.* **2013**, *25*, 5937−5942.

(15) Ju, J.; Yao, X.; Yang, S.; Wang, L.; Sun, R. Z.; He, Y. X.; Jiang, L. Cactus Stem Inspired Cone-Arrayed Surfaces for Efficient Fog Collection. *Adv. Funct. Mater.* **2014**, *24*, 6933−6938.

(16) Dong, H.; Wang, N.; Wang, L.; Bai, H.; Wu, J.; Zheng, Y. M.; Zhao, Y.; Jiang, L. Bioinspired Electrospun Knotted Microfibers for Fog Harvesting. *ChemPhysChem* **2012**, *13*, 1153−1156.

(17) Tian, X. L.; Chen, Y.; Zheng, Y. M.; Bai, H.; Jiang, L. Controlling Water Capture of Bioinspired Fibers with Hump Structures. *Adv. Mater.* **2011**, *23*, 5486−5491.

(18) Bai, H.; Ju, J.; Zheng, Y. M.; Jiang, L. Functional Fibers with Unique Wettability Inspired by Spider Silks. *Adv. Mater.* **2012**, *24*, 2786−2791.

(19) Zhai, L.; Berg, M. C.; Cebeci, F. C.; Kim, Y.; Milwid, J. M.; Rubner, M. F.; Cohen, R. E. Patterned superhydrophobic surfaces: Toward a synthetic mimic of the Namib Desert beetle. *Nano Lett.* **2006**, *6*, 1213−1217.

(20) Ishii, D.; Yabu, H.; Shimomura, M. Novel Biomimetic Surface Based on a Self-Organized Metal-Polymer Hybrid Structure. *Chem. Mater.* **2009**, *21*, 1799−1801.

(21) Chen, R. G.; Zhang, X. G.; Su, Z. H.; Gong, R.; Ge, X.; Zhang, H. J.; Wang, C. Perfectly Hydrophobic Silicone Nanofiber Coatings: Preparation from Methyltrialkoxysilanes and Use as Water-Collecting Substrate. *J. Phys. Chem. C* **2009**, *113*, 8350−8356.

(22) Thickett, S. C.; Neto, C.; Harris, A. T. Biomimetic Surface Coatings for Atmospheric Water Capture Prepared by Dewetting of Polymer Films. *Adv. Mater.* **2011**, *23*, 3718−3722.

(23) Wang, B.; Zhang, Y. B.; Liang, W. X.; Wang, G. Y.; Guo, Z. G.; Liu, W. M. A simple route to transform normal hydrophilic cloth into a superhydrophobic-superhydrophilic hybrid surface. *J. Mater. Chem. A* **2014**, *2*, 7845−7852.

(24) Bai, H.; Wang, L.; Ju, J.; Sun, R. Z.; Zheng, Y. M.; Jiang, L. Efficient Water Collection on Integrative Bioinspired Surfaces with Star-Shaped Wettability Patterns. *Adv. Mater.* **2014**, *26*, 5025−5030.

(25) Wenzel, R. N. Resistance of solid surfaces to wetting by water. *Ind. Eng. Chem.* **1936**, *28*, 988−994.

(26) Liu, Y. Y.; Chen, X. Q.; Xin, J. H. Can superhydrophobic surfaces repel hot water? *J. Mater. Chem.* **2009**, *19*, 5602−5611.

(27) Chen, X. Q.; Liu, Y. Y.; Lu, H. F.; Yang, H. R.; Zhou, X. A.; Xin, J. H. In-situ growth of silica nanoparticles on cellulose and application of hierarchical structure in biomimetic hydrophobicity. *Cellulose* **2010**, *17*, 1103−1113.

(28) Wang, R.; Hashimoto, K.; Fujishima, A.; Chikuni, M.; Kojima, E.; Kitamura, A.; Shimohigoshi, M.; Watanabe, T. Light-induced amphiphilic surfaces. *Nature* **1997**, *388*, 431−432.

(29) Kong, Y. Y.; Liu, Y. Y.; Xin, J. H. Fabrics with self-adaptive wettability controlled by "light-and-dark". *J. Mater. Chem.* **2011**, *21*, 17978−17987.

(30) Emeline, A. V.; Rudakova, A. V.; Sakai, M.; Murakami, T.; Fujishima, A. Factors Affecting UV-Induced Superhydrophilic Conversion of a TiO2 Surface. *J. Phys. Chem. C* **2013**, *117*, 12086−12092.

(31) Neuvonen, S.; Suomela, J. The effect of simulated acid rain on pine needle and birch leaf litter decomposition. *J. Appl. Ecol.* **1990**, *27*, 857−872.

(32) Franklin, W. E.; Rowland, S. P. Thermogravimetric Analysis and Pyrolysis Kinetics of Cotton Fabrics Finished with Thpoh-Nh3. *J. Macromol. Sci., Chem.* **1983**, *19*, 265−282.

DOI: 10.1021/acsami.5b08941
ACS Appl. Mater. Interfaces 2016, 8, 2950−2960

(33) Price, D.; Horrocks, A. R.; Akalin, M.; Faroq, A. A. Influence of flame retardants on the mechanism of pyrolysis of cotton (cellulose) fabrics in air. *J. Anal. Appl. Pyrolysis* **1997**, *40*−*41*, 511−524.

DOI: 10.1021/acsami.5b08941
ACS Appl. Mater. Interfaces 2016, 8, 2950−2960